On the Throughput of Full-duplex MIMO in the Multi-link Case

Diep N. Nguyen[1] and Marwan Krunz[2] and Stephen Hanly[1]
[1]Department of Engineering, Macquarie University, Australia
E-mail:{diep.nguyen, stephen.hanly}@mq.edu.au
[2]Department of Electrical and Computer Engineering, University of Arizona, USA
E-mail:{krunz}@email.arizona.edu

***Abstract*—We are concerned with the throughput of a full-duplex (FD) MIMO network. Unlike conventional half-duplex (HD) MIMO, two wireless devices of a bidirectional FD-MIMO link have freedom of selecting which antennas/RF-chains to transmit or receive before tuning their radiation patterns to maximize the link's throughput. The freedom in configuring the function of available RF-chains, resulting in various FD-MIMO transmission modes, is referred to as *FD-MIMO freedom* that is shown to significantly improve the spectral efficiency of a given link. For a given RF-chain/antenna selection of a set of FD-MIMO links, we end up with a non-convex throughput maximization problem of a heterogeneous MIMO network. We design both centralized (using the augmented Lagrange function) and distributed algorithm (using a hierarchical game and pricing) to solve the problem for its locally optimal solutions. Comparing the achieved throughput of the FD-MIMO network, averaged over all obtained locally optimal solutions, with that when FD-MIMO nodes choose to operate in an HD mode, we find the HD mode surprisingly outperforms the FD mode. This trend is also observed when exploring all possible communication modes of a small size FD-MIMO network.**

***Index Terms*—Spectral efficiency, full-duplex, MIMO, beamforming, Nash equilibrium, nonconvex optimization.**

I. Introduction

It has been recently demonstrated that a wireless device can transmit and receive simultaneously, i.e., perform full-duplex (FD) communications, on the same channel [1] [2]. The resulting link throughput is nearly double that of a conventional half-duplex (HD) link [3]. FD communications is enabled through various self-interference suppression (SIS) techniques, including antenna cancelation, RF cancelation and digital cancelation [1] [2]. Interested readers are referred to [3] and the references therein for the latest development on SIS. Perfect SIS, i.e., completely bringing self-interference to the noise floor level (110 dB reduction), has been demonstrated in [3]. Various works have shown significant throughput improvements of FD over HD communications for a *single* link [1] [4] [3]. The spectral efficiency can be further boosted when combining SIS with multi-input multi-output (MIMO) technology [5]. In this article, we study the implications of FD-MIMO in network designs. Specifically, we are interested in answering: in a *network* context, how much spectral efficiency improvement, if any, can FD-MIMO provide compared with HD-MIMO?

An FD-MIMO transceiver with SIS capability can be exploited in two ways: FD-MIMO relaying or FD-MIMO bidirectional channels. In the former, a node receives data from another node and simultaneously transmits data to a third node. In our work, we consider a network of bidirectional FD-MIMO links. The first FD-MIMO design [5], MIDU, used two separate antenna arrays at each node to transmit and to receive, so that MIMO is enabled in both forward and reverse directions. Note that a FD-MIMO device that transmits and receives on *the same antenna array* is not yet possible at the time of this work due to the cross-antenna interference [3]. However, with the latest development in SIS [3] that allows an antenna to transmit and receive simultaneously, a FD-MIMO link now has the freedom of selecting which antennas/RF-chains to transmit or receive on (but not both) in the forward and reverse directions.

More specifically, consider a pair of FD-MIMO devices, each with M antennas. For each of the M data streams between both ends, we have freedom to choose which antenna to start from and which antenna to terminate at. For $M = 4$, Figure 1(a) illustrates a FD-MIMO link with undecided Tx/Rx antennas that can be of various possibilities, including but not limited to: 2×2 FD-MIMO (Figure 1(b)), 1×3 FD-MIMO (Figure 1(c)), or even 4×4 HD-MIMO (Figure 1(d)). Here, the $x \times y$ FD-MIMO configuration refers to $x \times x$ and $y \times y$ HD-MIMO mode on the forward and reverse directions. Additionally, a given FD-MIMO configuration can be realized via different antenna selections that result in different performance (e.g., both Figures 1(b) and (e) realize 2×2 FD-MIMO; Figure 1(c) and (f) for 1×3 FD-MIMO). In a network context, the FD Tx/Rx antenna selection can also be helpful in reducing network interference (e.g., Tx antennas should be ones that induce less network interference) as well as mitigating interference effect (e.g., Rx antennas should be ones that are less interfered from others), consequently improving network throughput. We refer such freedom in configuring FD-MIMO operational modes as *FD-MIMO freedom*. The first hardware radio that supports FD-MIMO freedom has been recently demonstrated [6].

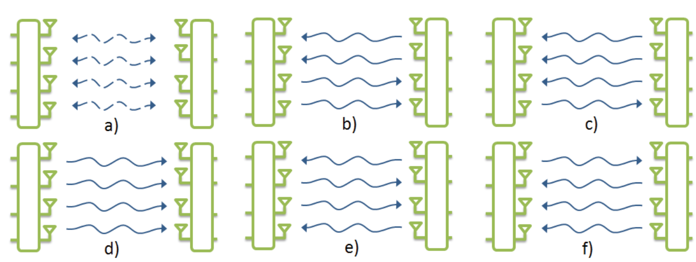

Fig. 1. Freedom in selecting different FD-MIMO configurations.

The ultimate goal of our paper is to investigate the spectral efficiency of FD-MIMO under a network context with optimal Tx/Rx antenna selection. Such a FD-MIMO network consists of various FD-MIMO links, operating with different FD-MIMO configurations (possibly including HD-MIMO mode). Note that most existing works on FD communications investigated single-link scenarios. Specifically, the suboptimal throughput of a single FD-MIMO relaying and bidirectional channels was visited in [7] and [8], respectively. The tradeoff between diversity and

This research was supported in part by the National Science Foundation (grants IIP-1265960 and IIP-1231043), the CSIRO Macquarie University Chair in Wireless Communications. This Chair has been established with funding provided by the Science and Industry Endowment Fund. Any opinions, findings, conclusions, or recommendations expressed in this paper are those of the author(s) and do not necessarily reflect the views of the National Science Foundation.

multiplexing gain of a single FD-MIMO relaying channel was explored in [9]. In [5], the authors showed that FD-MIMO significantly improves the link throughput, compared with HD-MIMO.

The network-throughput maximization problem of FD-MIMO involves both binary variables of antenna selection and continuous variables of MIMO *precoding matrices* which control antenna radiation patterns. Even if we fix the antenna selection, we still end up with a non-convex throughput maximization problem of a heterogeneous MIMO network. To tackle it, we transfer the problem into a hierarchical game in which the forward and reverse links of a bidirectional FD link first cooperate in determining the set of transmit and receive antennas. In the second stage, each bidirectional FD-MIMO link participates in a noncooperative game, aiming at maximizing its own throughput. We design a pricing policy for each FD-MIMO node, which drives the noncooperative game to a Nash-Equilibrium (NE). The network throughput under this NE equals to that of a locally optimal solution of the non-convex centralized problem.

Simulations show that the network throughput under the distributed algorithm rapidly converges to that of the centralized one. Comparing the achieved throughput of the FD-MIMO network with that when FD-MIMO nodes choose to operate in HD mode with all of its antennas, the HD mode often surprisingly outperforms the FD mode. This trend is also observed when we explore all possible communication modes of a small-size FD-MIMO network. The above observation is somehow counterintuitive as for the single link case, FD-MIMO generally performs much better than HD-MIMO. However, it can be justified by noting that for interfering links, HD-MIMO has three advantages that can make it preferable to FD-MIMO. First, a link that operates in HD mode is likely to inject less interference into the network, compared with FD-MIMO in which both ends of a link are transmitting. Second, when a FD-MIMO node uses all of its available antennas to operate as a HD-MIMO transmitter, it has more freedom to tune its radiation pattern to avoid interfering with nearby unintended receivers. This consequently reduces the multi-user interference and improves network throughput. Third, a network with more links operating at HD-mode has less unintended receivers, giving more interference-free directions for other MIMO transmitters to beamform to their intended receivers.

Throughout the paper, we use $(.)^*$ to denote the conjugate of a matrix, $(.)^H$ to denote its Hermitian transpose, tr$(.)$ for the trace of a matrix, $|.|$ for the matrix determinant or a set's cardinality, and $(.)^T$ for the matrix transpose. diag$_s(.)$ indicates the diagonal element (s,s) of a matrix. sum$(.)$ gives the summation of all elements of a vector. Matrices, vectors, and sets are bold-faced.

II. Network Model

Consider a network of N FD-MIMO links (i.e., $2N$ FD-MIMO nodes), denoted by set $\mathbf{\Phi} \stackrel{\text{def}}{=} \{1,\dots,N\}$. Each node is equipped with M antennas, each of which can be configured to transmit or receive, but not at the same time[1]. Let $\mathbf{s}_u^f(:)$ be a $1\times M$ vector with $\mathbf{s}_u^f(i)=1$ if the ith antenna of the transmitter of the forward direction of a bidirectional FD link u serves as a transmit antenna, otherwise (i.e., $\mathbf{s}_u^f(i)=0$) i is a receive antenna (for the reverse direction). Note that the forward and reverse directions are selected arbitrarily. Vector $\mathbf{s}_u^r(:)$ is defined in a similar way for the reverse direction of link u.

Let $\mathbf{H}_{uu}^f$ ($\mathbf{H}_{uu}^r$) denote the $M\times M$ channel gain matrix of the forward (reverse) direction of link u when the link operates in HD mode. It is clear that $\mathbf{H}_{uu}^f$ is the transpose of $\mathbf{H}_{uu}^r$. Each element of $\mathbf{H}_{uu}^f$ is a multiplication of a distance- and channel-dependent attenuation term and a random term that reflects multi-path fading (complex Gaussian variables with zero mean and unit variance). Let $\mathbf{H}_{uv}^{ff}$ ($\mathbf{H}_{uv}^{fr}$) denote the $M\times M$ interfering channel gain matrix from the transmitter of forward (reverse) direction of link v to the receiver of forward direction of link u in HD mode.

For a given selection of Tx/Rx antennas ($\mathbf{s}_u^r(:)$ and $\mathbf{s}_u^f(:)$, $\forall u=1,\dots,N$) at all FD-MIMO nodes, the resulting channel gain matrix between any two nodes consists of a subset of M^2 elements of the corresponding HD channel gain matrix. Specifically, let $\mathbf{e}_i$ be a $1\times M$ vector of the standard basis of M-dimension Euclidean space of which the ith element is 1 and all others are 0. The channel gain matrix $\mathbf{h}_{uu}^f$ of the forward direction of link u is:

$$\mathbf{h}_{uu}^f = \mathbf{L}_u^f \mathbf{H}_{uu}^f \mathbf{R}_u^f \tag{1}$$

where:

$$\begin{aligned}
\mathbf{L}_u^f &= [\mathbf{e}_{\pi(1)}^T,\dots,\mathbf{e}_{\pi(t)}^T,\dots,\mathbf{e}_{\pi(|\mathbf{S}^r|)}^T],\\
&\quad \text{with } \mathbf{S}^r \stackrel{\text{def}}{=} \{\pi(t)\} = \{1\le j\le M | s_u^r(j)=0\}\\
\mathbf{R}_u^f &= [\mathbf{e}_{\pi(1)}^T,\dots,\mathbf{e}_{\pi(t)}^T,\dots,\mathbf{e}_{\pi(|\mathbf{T}^f|)}^T]^T\\
&\quad \text{with } \mathbf{T}^f \stackrel{\text{def}}{=} \{\pi(t)\} = \{1\le j\le M | s_u^f(j)=1\}.
\end{aligned} \tag{2}$$

Similarly, the channel gain matrix $\mathbf{h}_{uu}^r$ of the reverse direction of link u is:

$$\mathbf{h}_{uu}^r = \mathbf{L}_u^r \mathbf{H}_{uu}^r \mathbf{R}_u^r \tag{3}$$

where:

$$\begin{aligned}
\mathbf{L}_u^r &= [\mathbf{e}_{\pi(1)}^T,\dots,\mathbf{e}_{\pi(t)}^T,\dots,\mathbf{e}_{\pi(|\mathbf{S}^f|)}^T],\\
&\quad \text{with } \mathbf{S}^f \stackrel{\text{def}}{=} \{\pi(t)\} = \{1\le j\le M | s_u^f(j)=0\}\\
\mathbf{R}_u^r &= [\mathbf{e}_{\pi(1)}^T,\dots,\mathbf{e}_{\pi(t)}^T,\dots,\mathbf{e}_{\pi(|\mathbf{T}^r|)}^T]^T\\
&\quad \text{with } \mathbf{T}^r \stackrel{\text{def}}{=} \{\pi(t)\} = \{1\le j\le M | s_u^r(j)=1\}.
\end{aligned} \tag{4}$$

The interfering channel gain matrices $\mathbf{h}_{uv}^{ff}$ and $\mathbf{h}_{uv}^{fr}$ from the transmitters of forward and reverse directions of link v to the receiver of the forward direction of link u are:

$$\begin{aligned}
\mathbf{h}_{uv}^{ff} &= \mathbf{L}_u^f \mathbf{H}_{uv}^f \mathbf{R}_v^f\\
\mathbf{h}_{uv}^{fr} &= \mathbf{L}_u^f \mathbf{H}_{uv}^f \mathbf{R}_v^r
\end{aligned} \tag{5}$$

Other interfering channel matrices ($\mathbf{h}_{vu}^{rf}$ and $\mathbf{h}_{vu}^{rr}$) at the receiver of the reverse link v are found in a similar way. Note that although matrices $\mathbf{H}_{uu}^r$, $\mathbf{H}_{uu}^f$, and $\mathbf{H}_{uv}^{ff}$ have the same size $M\times M$, the resulting channel gain matrices (after Tx/Rx antenna selection) $\mathbf{h}_{uu}^f$, $\mathbf{h}_{uu}^r$, and $\mathbf{h}_{uv}^{ff}$ have different sizes. Additionally, as we want to harvest the spatial multiplexing gain (the minimum of the number of Tx and Rx antennas), it is not helpful to have an unequal number of Tx and Rx antennas. In other words, $\mathbf{h}_{uu}^f$ and $\mathbf{h}_{uu}^r$ are square matrices of size $sum(\mathbf{s}_u^f(:))\times sum(\mathbf{s}_u^f(:))$ and $sum(\mathbf{s}_u^r(:))\times sum(\mathbf{s}_u^r(:))$, respectively. $\mathbf{h}_{uv}^{ff}$ is not necessarily square and of size $sum(\mathbf{s}_u^f(:))\times sum(\mathbf{s}_v^f(:))$. Let $\mathbf{G}_u^f$ and $\mathbf{G}_u^r$ denote the precoding matrices of the forward and reverse directions of link u, respectively. $\mathbf{x}_u^f$ denotes the vector of information symbols being placed on the transmitter's antennas of the forward direction of link u. Then, the received signal vector $\mathbf{y}_u^f$ at the receiver of the forward direction of link u is:

[1]Due to cross-antenna interference, the SIS technique in [3] does not enable an antenna array to transmit and receive simultaneously [3].

$$
\begin{aligned}
\mathbf{y}_u^f =& \mathbf{h}_{uu}^f \mathbf{G}_u^f \mathbf{x}_u^f + \sum_{v \in \{\mathbf{\Phi} \backslash u\}} \mathbf{h}_{uv}^f \mathbf{G}_v^f \mathbf{x}_v^f \mathbb{1}_+[sum(\mathbf{s}_v^f(:))] \\
&+ \sum_{v \in \{\mathbf{\Phi} \backslash u\}} \mathbf{h}_{uv}^r \mathbf{G}_v^r \mathbf{x}_v^r \mathbb{1}_+[sum(\mathbf{s}_v^r(:))] + \mathbf{N}_{sum(\mathbf{s}_u^f(:))}
\end{aligned} \tag{6}
$$

where the first term is the intended signal, the second and third terms represent interference from transmitters of forward and reverse directions of link v (if their number of transmit antennas are not zero). $\mathbf{N}_{sum(\mathbf{s}_u^f(:))}$ is an $sum(\mathbf{s}_u^f(:)) \times 1$ complex Gaussian noise vector with identity covariance matrix $\mathbf{I}_{sum(\mathbf{s}_u^f(:))}$, representing the floor noise. $\mathbb{1}_+(z)$ is an indicator function that equals 1 if $z > 0$ and 0 otherwise. Note that we are assuming perfect SIS, meaning that there is no interference between forward and reverse directions of a given FD link. For cases with imperfect SIS, the FD-MIMO network throughput should be lower. Let c_u^f (c_u^r) denote the throughput of the forward (reverse) direction of link u if it is active, i.e., $sum(\mathbf{s}_u^f(:)) > 0$ ($sum(\mathbf{s}_u^r(:)) > 0$). Throughput of FD-MIMO link u, c_u, is:

$$
\begin{aligned}
c_u =& c_u^f + c_u^r = \log |\mathbf{I}_{sum(\mathbf{s}_u^f)} + \mathbf{G}_u^{fH} \mathbf{h}_{uu}^{fH} \mathbf{Q}_u^{f^{-1}} \mathbf{h}_{uu}^f \mathbf{G}_u^f| \\
&+ \log |\mathbf{I}_{sum(\mathbf{s}_u^r)} + \mathbf{G}_u^{rH} \mathbf{h}_{uu}^{rH} \mathbf{Q}_u^{r^{-1}} \mathbf{h}_{uu}^r \mathbf{G}_u^r|
\end{aligned} \tag{7}
$$

where $\mathbf{Q}_u^f$ is the noise-plus-interference covariance matrix at the receiver of forward direction of link u:

$$
\begin{aligned}
\mathbf{Q}_u^f = \mathbf{I}_{sum(\mathbf{s}_u^f(:))} &+ \sum_{v \in \{\mathbf{\Phi} \backslash u\}} \mathbf{h}_{uv}^{ff} \mathbf{G}_v^f \mathbf{G}_v^{fH} \mathbf{h}_{uv}^{ffH} \mathbb{1}_+[sum(\mathbf{s}_v^f(:))] \\
&+ \sum_{v \in \{\mathbf{\Phi} \backslash u\}} \mathbf{h}_{uv}^{fr} \mathbf{G}_v^r \mathbf{G}_v^{rH} \mathbf{h}_{uv}^{frH} \mathbb{1}_+[sum(\mathbf{s}_v^r(:))]
\end{aligned} \tag{8}
$$

The network throughput of a FD-MIMO network that depends on both the selection of Tx/Rx antennas *and* precoding matrices at each link u is formally written as:

$$
\begin{aligned}
&\underset{\{\mathbf{G}_u^f, \mathbf{G}_u^r, \mathbf{s}_u^f, \mathbf{s}_u^r, \forall u\}}{\text{maximize}} \sum_{u \in \mathbf{\Phi}} \left(c_u^f \mathbb{1}_+[sum(\mathbf{s}_u^f(:))] + c_u^r \mathbb{1}_+[sum(\mathbf{s}_u^r(:))] \right) \\
&\text{s.t.} \\
&\text{C1:} \quad sum(\mathbf{s}_u^f) + sum(\mathbf{s}_u^r) = M, \ \forall u \\
&\text{C2:} \quad \text{tr}(\mathbf{G}_u^f \mathbf{G}_u^{fH}) \le P_{\max}(u), \ \forall u \\
&\text{C3:} \quad \text{tr}(\mathbf{G}_u^r \mathbf{G}_u^{rH}) \le P_{\max}(u), \ \forall u.
\end{aligned} \tag{9}
$$

Note that constraint $C1$ also includes the possibility that a node does not want to use some of its antennas to avoid interfering with others. In such a case, the power allocated to these antennas is zero and set by configuring the corresponding precoding matrix.

Problem (9) is a mixed integer programming problem (MIPP), involving binary variables of antenna selection and continuous variables of MIMO precoders. This type of problem is known to be NP-hard. Solving (9) for the optimal solution is difficult. Even if we enumerate all Tx/Rx antenna combinations (2^{MN} cases), one still faces a non-convex throughput maximization of a heterogeneous MIMO network with both FD and HD links:

$$
\begin{aligned}
&\underset{\{\mathbf{G}_u^f, \mathbf{G}_u^r \forall u\}}{\text{maximize}} \sum_{u \in \mathbf{\Phi}} \left(c_u^f \mathbb{1}_+[sum(\mathbf{s}_u^f(:))] + c_u^r \mathbb{1}_+[sum(\mathbf{s}_u^r(:))] \right) \\
&\text{s.t.} \\
&\text{C2:} \quad \text{tr}(\mathbf{G}_u^f \mathbf{G}_u^{fH}) \le P_{\max}(u), \ \forall u \\
&\text{C3:} \quad \text{tr}(\mathbf{G}_u^r \mathbf{G}_u^{rH}) \le P_{\max}(u), \ \forall u.
\end{aligned} \tag{10}
$$

Before casting (9) as a hierarchical game that is amenable to distributed implementation, we develop a centralized algorithm that finds locally optimal solutions of the non-convex problem (10). This algorithm serves as a performance benchmark for distributed algorithm and provide a truely optimal solution to (9) when exhaustive search is applied to small size FD-MIMO networks.

III. Centralized Algorithm

In this section, we use the augmented Lagrange multiplier method to derive the centralized algorithm. For that purpose, problem (10) can be rewritten:

$$
\begin{aligned}
&\underset{\{\mathbf{G}_u^f, \mathbf{G}_u^r \forall u\}}{\text{minimize}} \sum_{u \in \mathbf{\Phi}} \left(-c_u^f \mathbb{1}_+[sum(\mathbf{s}_u^f(:))] - c_u^r \mathbb{1}_+[sum(\mathbf{s}_u^r(:))] \right) \\
&\text{s.t.} \\
&\text{C2:} \quad q_u^f = \text{tr}(\mathbf{G}_u^f \mathbf{G}_u^{fH}) - P_{\max}(u) \le 0, \ \forall u \\
&\text{C3:} \quad q_u^r = \text{tr}(\mathbf{G}_u^r \mathbf{G}_u^{rH}) - P_{\max}(u) \le 0, \ \forall u.
\end{aligned} \tag{11}
$$

Algorithm 1 : Centralized Algorithm

Initialize
$\mathbf{G}_u^f \leftarrow \mathbf{I}, \mathbf{G}_u^r \leftarrow \mathbf{I}, \forall u$
while $true$ **do**
  $\beta \leftarrow .7, \sigma \leftarrow .1$ (*%used in Armijo search*)
  $\gamma_u^f \leftarrow 0, \gamma_u^r \leftarrow 0, \forall u$
  $p \leftarrow 1$
  while $\partial L(\mathbf{G}_u^f, \mathbf{G}_u^r, \gamma_u^f, \gamma_u^r, p) \neq 0$ **do**
    $step \leftarrow 0.1$
    $D \leftarrow \partial L(\mathbf{G}_u^f, \mathbf{G}_u^r, \gamma_u^f, \gamma_u^r, p)$
    $d \leftarrow -step \times D; m \leftarrow 0$
    (*%find Armijo step size*)
    while $L(\mathbf{G}_u^f, \mathbf{G}_u^r, \gamma_u^f, \gamma_u^r, p) - L(\mathbf{G}_u^f + d, \mathbf{G}_u^r + d, \gamma_u^f, \gamma_u^r, p) \le -\sigma \beta^m step \partial L D$ **do**
      $step \leftarrow step \times \beta; m \leftarrow m + 1$
      $d \leftarrow -step \times D$
    end while
    $\mathbf{G}_u^f \leftarrow \mathbf{G}_u^f + d$; $\mathbf{G}_u^r \leftarrow \mathbf{G}_u^r + d$
  end while
  if $\max(q_u^f, q_u^r, \forall u) \le 0$ **break**
  $\forall u$:
  $\gamma_u^f = \gamma_u^f + pq_u^f$ **if** $\gamma_u^f + pq_u^f \ge 0$ **else** $\gamma_u^f = 0$
  $\gamma_u^r = \gamma_u^r + pq_u^r$ **if** $\gamma_u^r + pq_u^r \ge 0$ **else** $\gamma_u^r = 0$
  $p \leftarrow p \times \mu$ (*%$\mu \ge 1$, increase cost of violation*)
end while
Return $\mathbf{G}_u^f$**,** $\mathbf{G}_u^r$**,** $\forall u$

The augmented Lagrange [10] of (11) is given in (12) (next page), where p is a positive penalty parameter (for violating the constraints), γ_u^f, and γ_u^r are nonnegative Lagrangian multipliers. At a local optimal solution, (13) and (14) hold. The first, second, and third terms in (13) are:

$$
\begin{aligned}
&\frac{\partial c_v^f}{\partial \mathbf{G}_u^{f*}} = \\
&- \mathbf{h}_{vu}^{ffH} \mathbf{Q}_v^{f^{-1}} \mathbf{h}_{vu}^{ff} \mathbf{G}_u^f + \mathbf{h}_{vu}^{ffH} (\mathbf{Q}_v^f + \mathbf{h}_{vu}^{ff} \mathbf{G}_v^f \mathbf{G}_v^{fH} \mathbf{h}_{vu}^{ffH})^{-1} \mathbf{h}_{vu}^{ff} \mathbf{G}_u^f \\
&\frac{\partial c_v^r}{\partial \mathbf{G}_u^{f*}} = \\
&- \mathbf{h}_{vu}^{rfH} \mathbf{Q}_v^{r^{-1}} \mathbf{h}_{vu}^{rf} \mathbf{G}_u^f + \mathbf{h}_{vu}^{rfH} (\mathbf{Q}_v^r + \mathbf{h}_{vu}^{rf} \mathbf{G}_v^r \mathbf{G}_v^{rH} \mathbf{h}_{vu}^{rfH})^{-1} \mathbf{h}_{vu}^{rf} \mathbf{G}_u^f \\
&\frac{\partial c_u^f}{\partial \mathbf{G}_u^{f*}} = \mathbf{h}_{uu}^{fH} (\mathbf{Q}_u^f + \mathbf{h}_{uu}^f \mathbf{G}_u^f \mathbf{G}_u^{fH} \mathbf{h}_{uu}^{fH})^{-1} \mathbf{h}_{uu}^f \mathbf{G}_u^f.
\end{aligned} \tag{17}
$$

Since q_u^f and q_u^r are continuously differentiable w.r.t. every entry of $\mathbf{G}_u^f$, the fourth and fifth terms in (13) are also continuously differentiable [10]. Their derivatives are as follows:

$$
\frac{\partial \{(\max\{0, \gamma_u^f + pq_u^f\})^2\}}{\partial \mathbf{G}_u^f} = \begin{cases} 0 & \text{if } \gamma_u^f + pq_u^f \le 0 \\ 2p(\gamma_u^f + pq_u^f)\mathbf{G}_u^f & \end{cases}
$$

$$L(\mathbf{G}_u^f,\mathbf{G}_u^r,\gamma_u^f,\gamma_u^r,p)=-\sum_{u\in\mathbf{\Phi}}\Big(c_u^f-\frac{p}{2}\{(\max\{0,\gamma_u^f+pq_u^f\})^2-(\gamma_u^f)^2\}\Big)\,\mathbb{1}_+[sum(\mathbf{s}_u^f(:))] + \Big(c_u^r-\frac{p}{2}\{(\max\{0,\gamma_u^r+pq_u^r\})^2-(\gamma_u^r)^2\}\Big)\,\mathbb{1}_+[sum(\mathbf{s}_u^r(:))] \tag{12}$$

$$0=\frac{\partial L(\mathbf{G}_u^f,\mathbf{G}_u^r,\gamma_u^f,\gamma_u^r,p)}{\partial \mathbf{G}_u^{f*}}=-\sum_{v\in\{\mathbf{\Phi}\backslash u\}}\Big(\frac{\partial c_v^f}{\partial \mathbf{G}_u^{f*}}\mathbb{1}_+[sum(\mathbf{s}_v^f(:))]-\frac{\partial c_v^r}{\partial \mathbf{G}_u^{f*}}\mathbb{1}_+[sum(\mathbf{s}_v^r(:))]\Big)-\frac{\partial c_u^f}{\partial \mathbf{G}_u^{f*}}+\frac{p}{2}\frac{\partial\{(\max\{0,\gamma_u^f+pq_u^f\})^2-(\gamma_u^f)^2\}}{\partial \mathbf{G}_u^{f*}} +\frac{p}{2}\frac{\partial\{(\max\{0,\gamma_u^r+pq_u^r\})^2-(\gamma_u^r)^2\}}{\partial \mathbf{G}_u^{f*}} \tag{13}$$

$$0=\frac{\partial L(\mathbf{G}_u^f,\mathbf{G}_u^r,\gamma_u^f,\gamma_u^r,p)}{\partial \mathbf{G}_u^{r*}}=-\sum_{v\in\{\mathbf{\Phi}\backslash u\}}\Big(\frac{\partial c_v^f}{\partial \mathbf{G}_u^{r*}}\mathbb{1}_+[sum(\mathbf{s}_v^f(:))]-\frac{\partial c_v^r}{\partial \mathbf{G}_u^{r*}}\mathbb{1}_+[sum(\mathbf{s}_v^r(:))]\Big)-\frac{\partial c_u^r}{\partial \mathbf{G}_u^{r*}}+\frac{p}{2}\frac{\partial\{(\max\{0,\gamma_u^f+pq_u^f\})^2-(\gamma_u^f)^2\}}{\partial \mathbf{G}_u^{r*}} +\frac{p}{2}\frac{\partial\{(\max\{0,\gamma_u^r+pq_u^r\})^2-(\gamma_u^r)^2\}}{\partial \mathbf{G}_u^{r*}} \tag{14}$$

$$\boldsymbol{x}_u=\Big[\Re[vec(\mathbf{G}_u^f)]^T,\Re[vec(\mathbf{G}_u^r)]^T,\Im[vec(\mathbf{G}_u^f)]^T,\Im[vec(\mathbf{G}_u^r)]^T\Big]^T \tag{15}$$

$$\nabla_x L=2\Bigg[\Re[vec(\frac{\partial L}{\partial \mathbf{G}_1^{f*}})]^T,...,\Re[vec(\frac{\partial L}{\partial \mathbf{G}_N^{r*}})]^T,\Im[vec(\frac{\partial L}{\partial \mathbf{G}_1^{f*}})]^T,...,\Im[vec(\frac{\partial L}{\partial \mathbf{G}_N^{r*}})]^T\Bigg]^T \tag{16}$$

$$\frac{\partial\{(\max\{0,\gamma_u^r+pq_u^r\})^2\}}{\partial \mathbf{G}_u^f}\}=\begin{cases}0 & \text{if } \gamma_u^r+pq_u^r\le 0\\ 2p(\gamma_u^r+pq_u^r)\mathbf{G}_u^f\end{cases}$$

We use the gradient search algorithm with Armijo step size [10] to find $(\mathbf{G}_u^f,\mathbf{G}_u^r,\gamma_u^f,\gamma_u^r,p)$ such that (13) and (14) hold for forward and reverse directions of all links u. The details of the centralized algorithm are presented in Algorithm 1. We emphasize that the network throughput may vary from a locally optimal point to another. To account for this, we run the simulations with different initializations and take the average throughput. The running time for Algorithm 1 can be high as it involves NM^2 complex variables (or $2NM^2$ real ones). To implement Algorithm 1, we use the following isomorphism mapping from a complex matrix to a vector of real variables. The vector of variables $\boldsymbol{x}=[(\boldsymbol{x}_u^T)_{u=1}^N]^T$, with $\boldsymbol{x}_u$ in (15) and the corresponding Lagrange in (16).

IV. Hierarchical Game

We now cast (9) as a hierarchical game to design distributed algorithms.

A. Cooperative Phase: Tx/Rx Antenna Selection

In the first stage of the game, the forward and reverse directions of every FD-MIMO link cooperate in assigning Tx/Rx antennas. Specifically, the Tx antennas of the forward and reverse directions of FD-MIMO link u, vectors $\mathbf{s}_u^f$ and $\mathbf{s}_u^r$, are solution of the following problem:

$$\begin{aligned}&\underset{\{\mathbf{G}_u^f,\mathbf{G}_u^r,\mathbf{s}_u^f,\mathbf{s}_u^r\}}{\text{maximize}} \quad c_u\\ &\text{s.t.}\\ &\text{C1:}\quad sum(\mathbf{s}_u^f)+sum(\mathbf{s}_u^r)=M,\\ &\text{C2:}\quad \text{tr}(\mathbf{G}_u^f\mathbf{G}_u^{fH})\le P_{\max}(u),\\ &\text{C3:}\quad \text{tr}(\mathbf{G}_u^r\mathbf{G}_u^{rH})\le P_{\max}(u)\,.\end{aligned} \tag{18}$$

This is a binary programming problem which is NP-hard. Fortunately, for a moderate antenna array size, the total number of Tx/Rx antenna combinations ($\sum_{i=1}^{M} C(M,i)^2$) is not too large. For example, for $M=4$, the number of possible Tx/Rx combinations is 69. Moreover, for a given Tx/Rx antenna selection, (18) becomes a convex optimization problem which can be solved efficiently using standard methods [11]. Hence, it is possible to find the optimal Tx/Rx antenna selection for link u through exhaustive search. Note that in problem (18), both network interference (through noise-plus-interference covariance) from nearby transmitters and the channel state information (CSI) matrix of link u $\mathbf{H}_{uu}^r$ can be taken into account while selecting Tx/Rx antennas.

1) CSI-based Antenna Selection: Without interference (e.g., the protocol model or one active link in a collision domain), the matrices $\mathbf{Q}_u^f$ and $\mathbf{Q}_u^r$ in (18) reduce to identity matrices $\mathbf{I}_{sum(\mathbf{s}_u^f(:))}$ and $\mathbf{I}_{sum(\mathbf{s}_u^r(:))}$. Intuitively, the Tx/Rx antennas of FD link u are selected so that the HD channel gain matrix MIMO link u are "decomposed" into two "orthogonal" (forward and reverse) channels that have highest gains for each MIMO substream. For instance, consider the HD 4×4 channel gain matrix in (19). With SIS capability, the optimal Tx/Rx assignment are $\mathbf{s}_u^f=[1010]^T$ and $\mathbf{s}_u^r=[0101]^T$, meaning that the forward direction uses antennas 1st, 3rd to transmit and the reverse direction uses antennas 2nd, 4th to transmit. This forms two 2×2 MIMO channels on both directions.

For a single FD link with power budget of 50mW and bandwidth of 1Mhz, Figure 2(a) shows the throughput of FD-MIMO mode with/without optimal Tx/Rx antenna selection, compared with HD-MIMO mode. For FD-MIMO mode with fixed Tx/Rx antennas, we select, for example, the first antenna of both ends to acts as the Tx and Rx antennas for the forward direction while other antennas are used on the reverse direction. As can be seen, without Tx/Rx antenna selection, FD-MIMO mode does not offer significant throughput improvement over HD-MIMO mode. This observation agrees with findings in [5]. However, the FD-MIMO mode with optimal Tx/Rx antenna selection attains about 37% throughput higher than that of HD-MIMO mode.

$$\boldsymbol{H}_{11}^{f} = \begin{bmatrix} 0.4416+0.0016i & -0.1510-0.2037i & 0.0064+0.1185i & 0.0414-0.1225i \\ -0.0084+0.0390i & -0.1071-0.0857i & -0.0468+0.2139i & 0.2318+0.0158i \\ 0.1581+0.2587i & 0.2252-0.2657i & -0.2748-0.0920i & -0.0294+0.1495i \\ -0.4114+0.0715i & 0.2227+0.2623i & -0.0021-0.2105i & 0.0150+0.1718i \end{bmatrix} \tag{19}$$

$$L(\mathbf{G}_u^f, \mathbf{G}_u^r, \alpha_u^f, \alpha_u^r) = \sum_{u\in\boldsymbol{\Phi}} \Big[(c_u^f - \alpha_u^f(\text{tr}(\mathbf{G}_u^f \mathbf{G}_u^{fH}) - P_{\max}(u)))\mathbb{1}_+[sum(\mathbf{s}_u^f(:))] + (c_u^r - \alpha_u^r(\text{tr}(\mathbf{G}_u^r \mathbf{G}_u^{rH}) - P_{\max}(u)))\mathbb{1}_+[sum(\mathbf{s}_u^r(:))] \Big] \tag{20}$$

$$L_u(\mathbf{G}_u^f, \mathbf{G}_u^r, \alpha_u^f, \alpha_u^r) = (c_u^f - \alpha_u^f(\text{tr}(\mathbf{G}_u^f \mathbf{G}_u^{fH}) - P_{\max}(u))) + (c_u^r - \alpha_u^r(\text{tr}(\mathbf{G}_u^r \mathbf{G}_u^{rH}) - P_{\max}(u))) - \text{tr}\left(\mathbf{G}_u^{fH} \mathbf{A}_u^f \mathbf{G}_u^f\right) - \text{tr}\left(\mathbf{G}_u^{rH} \mathbf{A}_u^r \mathbf{G}_u^r\right) \tag{21}$$

$$\begin{aligned} \mathbf{A}_u^f = \sum_{v\in\{\boldsymbol{\Phi}\setminus u\}} &\Big(\mathbf{h}_{vu}^{ffH} \mathbf{Q}_v^{f\,-1} \mathbf{h}_{vv}^f [(\mathbf{G}_v^f \mathbf{G}_v^{fH})^{-1} + \mathbf{h}_{vv}^{fH} \mathbf{Q}_v^{f\,-1} \mathbf{h}_{vv}^f]^{-1} \mathbf{h}_{vv}^{fH} \mathbf{Q}_v^{f\,-1} \mathbf{h}_{vu}^{ff} \mathbb{1}_+[sum(\mathbf{s}_v^f(:))] \\ &+ \mathbf{h}_{vu}^{rfH} \mathbf{Q}_v^{r\,-1} \mathbf{h}_{vv}^r [(\mathbf{G}_v^r \mathbf{G}_v^{rH})^{-1} + \mathbf{h}_{vv}^{rH} \mathbf{Q}_v^{r\,-1} \mathbf{h}_{vv}^r]^{-1} \mathbf{h}_{vv}^{rH} \mathbf{Q}_v^{r\,-1} \mathbf{h}_{vu}^{rf} \mathbb{1}_+[sum(\mathbf{s}_v^r(:))] \Big) \\ \mathbf{A}_u^r = \sum_{v\in\{\boldsymbol{\Phi}\setminus u\}} &\Big(\mathbf{h}_{vu}^{frH} \mathbf{Q}_v^{f\,-1} \mathbf{h}_{vv}^f [(\mathbf{G}_v^f \mathbf{G}_v^{fH})^{-1} + \mathbf{h}_{vv}^{fH} \mathbf{Q}_v^{f\,-1} \mathbf{h}_{vv}^f]^{-1} \mathbf{h}_{vv}^{fH} \mathbf{Q}_v^{f\,-1} \mathbf{h}_{vu}^{fr} \mathbb{1}_+[sum(\mathbf{s}_v^f(:))] \\ &+ \mathbf{h}_{vu}^{rrH} \mathbf{Q}_v^{r\,-1} \mathbf{h}_{vv}^r [(\mathbf{G}_v^r \mathbf{G}_v^{rH})^{-1} + \mathbf{h}_{vv}^{rH} \mathbf{Q}_v^{r\,-1} \mathbf{h}_{vv}^r]^{-1} \mathbf{h}_{vv}^{rH} \mathbf{Q}_v^{r\,-1} \mathbf{h}_{vu}^{rr} \mathbb{1}_+[sum(\mathbf{s}_v^r(:))] \Big). \end{aligned} \tag{22}$$

2) CSI and Network Interference- based Antenna Selection: By accounting for interference from nearby transmitters, receivers of both directions can select antennas that are less interfered to be Rx antennas. However, since interference changes from this iteration to another due to the updates of MIMO precoding matrices, one needs to change its Rx (as well as Tx) antenna selection to adapt with the change in interference. The dynamic of Tx/Rx antennas over iterations makes it difficult to establish the existence of a NE as the per-link optimization problem with binary variables $\mathbf{s}_u^f$ and $\mathbf{s}_u^r$ is not convex [12].

We propose a sequential *antenna-alignment* process in which links sequentially solve problem (18) to determine their Tx/Rx assignment. Specifically, the first link selects its Tx/Rx antennas using only its HD CSI $\mathbf{H}_{uu}^r$ (or $\mathbf{H}_{uu}^f$). Upon perceiving interference from transmitters of both forward and reverse directions of the first link, the second link assigns its Tx/Rx antennas (by solving (18)), so on and so forth. After the last FD link finishes its Tx/Rx antenna selection, the Tx/Rx antenna assignment of all nodes are then fixed (i.e., only precoding matrices are updated) during the following iterations of the noncoopeartive phase. Note that the precoders obtained during the cooperative phase are used as the input/initializations in the noncooperative phase.

Figure 2(b) depicts network throughput (obtained using Algorithm 1) of FD-MIMO links in a square of $1000m \times 1000m$. As can be seen, taking network interference into the antenna-alignment process results in higher network throughput, compared with CSI-based antenna selection. Unlike the case of a single link in Figure 2(a), we observe that operating in FD-mode does not always lead to the highest throughput for a link under a network context. Instead, operating in HD-mode is the optimal choice for some links whose all antennas of a node are heavily interfered, hence should all operate in Tx mode.

B. Noncooperative Phase: Distributed Algorithm

As aforementioned, for a given Tx/Rx antenna selection found in the cooperative stage, we end up with the non-convex throughput maximization of a heterogeneous MIMO network with both FD and HD links (10). This non-convex problem is difficult to solve, even in a centralized manner. Centralized optimization solvers require exponential time w.r.t. the number of variables in the worst case. To design distributed algorithms that solve the network-wide problem (10), we reformulate (10) as a noncooperative game whose players are FD-MIMO links u. These players aim at maximizing their utilities, defined as links' throughput. The game's strategic space is the union of the strategic spaces of all players, shaped by constraints C2, C3 in (10). Each player/link u competes against others by selecting his strategic action of forward and reverse precoders $\mathbf{G}_u^f$, $\mathbf{G}_u^r$.

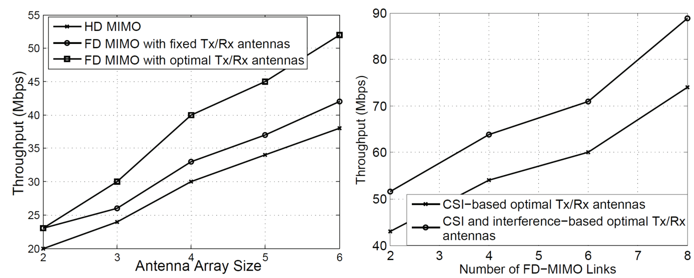

(a) Optimal vs. fixed antenna selection and HD-MIMO (one link).

(b) Optimal CSI-based vs. CSI and interference-based (a network).

Fig. 2. Throughput of FD-MIMO with optimal Tx/Rx antenna selection.

The payoff of player u, given below, is a function of its action $\mathbf{G}_u^f$, $\mathbf{G}_u^r$ as well as other players, defined as $\mathbf{G}_{-u}^f$, $\mathbf{G}_{-u}^r$ (captured by the forward and reverse noise-plus-interference covariance matrices $\mathbf{Q}_u^f$ and $\mathbf{Q}_u^r$ in c_u):

$$U_u(\mathbf{G}_u^f, \mathbf{G}_u^r, \mathbf{G}_{-u}^f, \mathbf{G}_{-u}^r) \stackrel{\text{def}}{=} c_u. \tag{23}$$

The transmitters of forward and reverse directions assign transmission power for each of selected Tx antennas and configure their radiation patterns to maximize the FD link's throughput. Formally, each FD link u solves the following problem for its optimal precoders:

$$\begin{aligned} &\underset{\{\mathbf{G}_u^f, \mathbf{G}_u^r\}}{\text{maximize}} \ U_u \\ &\text{s.t.} \\ &\text{C2:} \quad \text{tr}(\mathbf{G}_u^f \mathbf{G}_u^{fH}) \le P_{\max}(u), \\ &\text{C3:} \quad \text{tr}(\mathbf{G}_u^r \mathbf{G}_u^{rH}) \le P_{\max}(u), \ . \end{aligned} \tag{24}$$

To encourage MIMO transmitters of both directions steer their beam away from nearby receivers, the utility function of link u needs to account for interference that link u induces on nearby unintended receivers. We propose a pricing function that captures interference caused by transmitters of link u at unintended receivers. Intuitively, the higher the interference that link u causes, the more discount is applied to its utility function. For that purpose, new utility function of link u is written as:

$$U'_u(\mathbf{G}_u^f, \mathbf{G}_u^r, \mathbf{G}_{-u}^f, \mathbf{G}_{-u}^r) = c_u - F_u(\mathbf{G}_u^f, \mathbf{G}_u^r) \tag{25}$$

with the pricing function $F_u(\mathbf{G}_u^f, \mathbf{G}_u^r)$ for link u:

$$F_u(\mathbf{G}_u^f, \mathbf{G}_u^r) = \text{tr}\left(\mathbf{G}_u^{fH}\mathbf{A}_u^f\mathbf{G}_u^f\right) + \text{tr}\left(\mathbf{G}_u^{rH}\mathbf{A}_u^r\mathbf{G}_u^r\right) \tag{26}$$

where $\mathbf{A}_u^f$ is an $sum(\mathbf{s}_u^f(:)) \times sum(\mathbf{s}_u^f(:))$ positive-semidefinite matrix, referred to as the pricing-factor submatrix of the forward direction of link u. Similarly, the $sum(\mathbf{s}_u^r(:)) \times sum(\mathbf{s}_u^r(:))$ positive-semidefinite matrix $\mathbf{A}_u^r$ is referred to as the pricing-factor submatrix of the reverse direction of link u.

The noncooperative game among FD links with pricing is:

$$\begin{aligned} &\underset{\{\mathbf{G}_u^f, \mathbf{G}_u^r\}}{\text{maximize}} \;\; c_u - F_u(\mathbf{G}_u^f, \mathbf{G}_u^r) \\ &\text{s.t.} \\ &\text{C2:} \quad \text{tr}(\mathbf{G}_u^f\mathbf{G}_u^{fH}) \le P_{\max}(u), \\ &\text{C3:} \quad \text{tr}(\mathbf{G}_u^r\mathbf{G}_u^{rH}) \le P_{\max}(u), \; . \end{aligned} \tag{27}$$

The following theorem guarantees the existence of a NE of the game (27).

Theorem 1: The noncooperative game (27) admits at least one NE.

Proof: It is easy to verify that:

1) The action space of each player is convex and compact.
2) The utility function $U'_u(\mathbf{G}_u^f, \mathbf{G}_u^r, \mathbf{G}_{-u}^f, \mathbf{G}_{-u}^r)$ is concave w.r.t. $\mathbf{G}_u^f, \mathbf{G}_u^r$.

The NE existence follows [12]. □

We now derive a user-dependent pricing function that ensures at the resulting NE, the network throughput is at least as good as that of a locally optimal solution to the network optimization problem (10).

Theorem 2: If the pricing-factor matrices $\mathbf{A}_u^f$ and $\mathbf{A}_u^r$ are set as in (22). Then, the network throughput at a NE of the game (27) equals to that of a locally optimal solution of the network-wide problem (10).

Proof: The Lagrange function of the network throughput maximization (10) is in (20). The Lagrange function of the per-link optimization problem (27) of link u is in (21). Using similar steps in [13], the following equations force the K.K.T. conditions of the per-user optimization problem (27) to meet the K.K.T. conditions of the network-wide problem (10):

$$\begin{aligned} -\mathbf{A}_u^f\mathbf{G}_u^f &= \sum_{v\in\{\mathbf{\Phi}\backslash u\}} \Big(\frac{\partial c_v^f}{\partial \mathbf{G}_u^{f*}}\mathbb{1}_+[sum(\mathbf{s}_v^f(:))] + \frac{\partial c_v^r}{\partial \mathbf{G}_u^{f*}}\mathbb{1}_+[sum(\mathbf{s}_v^r(:))]\Big) \\ -\mathbf{A}_u^r\mathbf{G}_u^r &= \sum_{v\in\{\mathbf{\Phi}\backslash u\}} \Big(\frac{\partial c_v^f}{\partial \mathbf{G}_u^{r*}}\mathbb{1}_+[sum(\mathbf{s}_v^f(:))] + \frac{\partial c_v^r}{\partial \mathbf{G}_u^{r*}}\mathbb{1}_+[sum(\mathbf{s}_v^r(:))]\Big). \end{aligned} \tag{28}$$

Using equations in (17), we get (22). □

We now solve problem (27) for the optimal precoders of link u, i.e., best response. Observe that with perfect SIS, there is no leaked interference between both directions of the link. This fact is conveyed in the objective function of (27) which can be decomposed into two subproblems:

$$\begin{aligned} &\underset{\{\mathbf{G}_u^f\}}{\text{maximize}} \;\; c_u^f - \text{tr}\left(\mathbf{G}_u^{fH}\mathbf{A}_u^f\mathbf{G}_u^f\right) \\ &\text{s.t.} \\ &\text{C2:} \quad \text{tr}(\mathbf{G}_u^f\mathbf{G}_u^{fH}) \le P_{\max}(u), \end{aligned} \tag{29}$$

and

$$\begin{aligned} &\underset{\{\mathbf{G}_u^r\}}{\text{maximize}} \;\; c_u^r - \text{tr}\left(\mathbf{G}_u^{rH}\mathbf{A}_u^r\mathbf{G}_u^r\right) \\ &\text{s.t.} \\ &\text{C3:} \quad \text{tr}(\mathbf{G}_u^r\mathbf{G}_u^{rH}) \le P_{\max}(u), \end{aligned} \tag{30}$$

As the two problems have a similar structure and to save space, we briefly discuss the solution for the forward direction. Problem (29) is convex, hence can be solved efficiently (e.g., the interior-point method). Alternatively, one can rely on Hadamard inequality [14] and strong duality of convex optimization as in [15]. Specifically, the Lagrange function of (29) is:

$$\begin{aligned} L_u^f(\mathbf{G}_u^f, \beta_u^f) &= \log|\mathbf{I}_{sum(\mathbf{s}_u^f)} + \mathbf{G}_u^{fH}\mathbf{h}_{uu}^{fH}\mathbf{Q}_u^{f^{-1}}\mathbf{h}_{uu}^f\mathbf{G}_u^f| \\ &\quad - \alpha_u^f(\text{tr}(\mathbf{G}_u^f\mathbf{G}_u^{fH}) - P_{\max}(u)) - \text{tr}\left(\mathbf{G}_u^{fH}\mathbf{A}_u^f\mathbf{G}_u^f\right) \\ &= \log|\mathbf{I}_{sum(\mathbf{s}_u^f)} + \mathbf{G}_u^{fH}\mathbf{h}_{uu}^{fH}\mathbf{Q}_u^{f^{-1}}\mathbf{h}_{uu}^f\mathbf{G}_u^f| \\ &\quad - \text{tr}\left(\mathbf{G}_u^{fH}\left(\mathbf{A}_u^f + \beta_u^f\mathbf{I}_{sum(\mathbf{s}_u^f)}\right)\mathbf{G}_u^f\right) + \beta_u^f P_{\max}(u) \\ &= \log|\mathbf{I}_{sum(\mathbf{s}_u^f)} + \mathbf{G}_u^{fH}\mathbf{h}_{uu}^{fH}\mathbf{Q}_u^{f^{-1}}\mathbf{h}_{uu}^f\mathbf{G}_u^f| \\ &\quad - \text{tr}\left(\mathbf{G}_u^{fH}\mathbf{E}_u^f\mathbf{E}_u^{fH}\mathbf{G}_u^f\right) + \beta_u^f P_{\max}(u) \\ &= \log|\mathbf{I}_{sum(\mathbf{s}_u^f)} + \tilde{\mathbf{G}}_u^{fH}\mathbf{E}_u^{f^{-1}}\mathbf{h}_{uu}^{fH}\mathbf{Q}_u^{f^{-1}}\mathbf{h}_{uu}^f\mathbf{E}_u^{fH^{-1}}\tilde{\mathbf{G}}_u^f| \\ &\quad - \text{tr}\left(\tilde{\mathbf{G}}_u^{fH}\tilde{\mathbf{G}}_u^f\right) + \beta_u^f P_{\max}(u) \end{aligned} \tag{31}$$

where Cholesky decomposition of $\left(\mathbf{A}_u^f + \beta_u^f\mathbf{I}_{sum(\mathbf{s}_u^f)}\right) = \mathbf{E}_u^f\mathbf{E}_u^{fH}$ and $\tilde{\mathbf{G}}_u^{fH} = \mathbf{G}_u^{fH}\mathbf{E}_u^f$.

Besides its convexity, it is easy to verify that the Slater conditions hold for problem (29), i.e., strong duality holds for (29). Hence, its solution also maximizes its Lagrange. Using Hadamard inequality [14], we have (32). The inequality becomes an equality if we select $\mathbf{G}_u^f$ such that $\tilde{\mathbf{G}}_u^f$ is orthonormal and diagonalizes $\mathbf{E}_u^{f^{-1}}\mathbf{h}_{uu}^{fH}\mathbf{Q}_u^{f^{-1}}\mathbf{h}_{uu}^f\mathbf{E}_u^{fH^{-1}}$, equivalently:

$$\begin{aligned} &\tilde{\mathbf{G}}_u^{fH}\tilde{\mathbf{G}}_u^f = \mathbf{I} \\ &\tilde{\mathbf{G}}_u^{fH}\mathbf{E}_u^{f^{-1}}\mathbf{h}_{uu}^{fH}\mathbf{Q}_u^{f^{-1}}\mathbf{h}_{uu}^f\mathbf{E}_u^{fH^{-1}}\tilde{\mathbf{G}}_u^f = \mathbf{\Lambda}_u^f \end{aligned} \tag{33}$$

where $\mathbf{\Lambda}_u^f$ is a $sum(\mathbf{s}_v^f(:)) \times sum(\mathbf{s}_v^f(:))$ diagonal matrix.

By recalling $\tilde{\mathbf{G}}_u^{fH} = \mathbf{G}_u^{fH}\mathbf{E}_u^f$ and the Cholesky decomposition, we have:

$$\mathbf{h}_{uu}^{fH}\mathbf{Q}_u^{f^{-1}}\mathbf{h}_{uu}^f\mathbf{G}_u^f = [\mathbf{A}_u^f + \beta_u^f\mathbf{I}_{sum(\mathbf{s}_v^f(:))}]\mathbf{G}_i^{(k)}\mathbf{\Lambda}_i^{(k)}$$

or $\mathbf{G}_u^f$ is the generalized eigen matrix of $\mathbf{h}_{uu}^{fH}\mathbf{Q}_u^{f^{-1}}\mathbf{h}_{uu}^f$ and $[\mathbf{A}_u^f + \beta_u^f\mathbf{I}_{sum(\mathbf{s}_v^f(:))}]$ [16].

Note that if the unit-norm column matrix $\bar{\mathbf{G}}_u^f$ is a generalized eigen matrix of $\mathbf{h}_{uu}^{fH}\mathbf{Q}_u^{f^{-1}}\mathbf{h}_{uu}^f$ and $[\mathbf{A}_u^f + \beta_u^f\mathbf{I}_{sum(\mathbf{s}_v^f(:))}]$, so does any $\mathbf{G}_u^f$ of the form $\mathbf{G}_u^f = \bar{\mathbf{G}}_u^f\boldsymbol{P}_u^{f^{1/2}}$ [16] where $\boldsymbol{P}_u^f$ is a non-negative diagonal matrix. The complex matrix $\bar{\mathbf{G}}_u^f$ specifies the optimal directions of the radiation pattern of the forward transmitter of link u. Each non-negative element $\boldsymbol{P}_u^f(s)$ on diagonal of $\boldsymbol{P}_u^f$ specifies the optimal power allocated on antenna s of the forward direction of link u. As $\bar{\mathbf{G}}_u^f$ is a generalized eigen matrix of matrices $\mathbf{h}_{uu}^{fH}\mathbf{Q}_u^{f^{-1}}\mathbf{h}_{uu}^f$ and $[\mathbf{A}_u^f + \beta_u^f\mathbf{I}_{sum(\mathbf{s}_v^f(:))}]$, $\bar{\mathbf{G}}_u^f$ should diagonalize each of the two matrices [16]:

$$\begin{aligned} &\bar{\mathbf{G}}_u^{fH}[\mathbf{h}_{uu}^{fH}\mathbf{Q}_u^{f^{-1}}\mathbf{h}_{uu}^f]\bar{\mathbf{G}}_u^f = \mathbf{\Pi}_u^f \text{ and} \\ &\bar{\mathbf{G}}_u^{fH}[\mathbf{A}_u^f + \beta_u^f\mathbf{I}_{sum(\mathbf{s}_v^f(:))}]\bar{\mathbf{G}}_u^f = \mathbf{\Omega}_u^f \end{aligned} \tag{34}$$

where $\mathbf{\Pi}_u^f$ and $\mathbf{\Omega}_u^f$ are $sum(\mathbf{s}_v^f(:)) \times sum(\mathbf{s}_v^f(:))$ diagonal.

The Lagrange of (29) becomes:

$$\begin{aligned} &L_u^f(\mathbf{G}_u^f, \beta_u^f) = \\ &\sum_{s=1}^{sum(\mathbf{s}_v^f(:))}\Big(\log\left(1 + P_u^f(s)\text{diag}_s(\mathbf{\Pi}_u^f)\right) - P_u^f(s)\text{diag}_s(\mathbf{\Omega}_u^f)\Big) + \beta_u^f P_{\max}(u) \end{aligned} \tag{35}$$

$$L_u^f \leq \beta_u^f P_{\max}(u) - \mathrm{tr}\left(\tilde{\mathbf{G}}_u^{fH}\tilde{\mathbf{G}}_u^f\right) + \sum_{s=1}^{sum(\mathbf{s}_v^f(:))} \log(1+\mathrm{diag}_s\{\tilde{\mathbf{G}}_u^{fH}\mathbf{E}_u^{f^{-1}}\mathbf{h}_{uu}^{fH}\mathbf{Q}_u^{f^{-1}}\mathbf{h}_{uu}^{f}\mathbf{E}_u^{fH^{-1}}\tilde{\mathbf{G}}_u^f\}) \quad (32)$$

The optimal power allocation $P_u^f(s)$ should satisfy:

$$\frac{\partial L_u^f(\mathbf{G}_u^f, \beta_u^f)}{\partial P_u^f(s)} = \frac{\mathrm{diag}_s(\mathbf{\Pi}_u^f)}{1 + P_u^f(s)\mathrm{diag}_s(\mathbf{\Pi}_u^f)} - \mathrm{diag}_s(\mathbf{\Omega}_u^f) = 0 \quad (36)$$

Thus,

$$P_u^f(s) = \max\left(0, \frac{\mathrm{diag}_s(\mathbf{\Pi}_u^f) - \mathrm{diag}_s(\mathbf{\Omega}_u^f)}{\mathrm{diag}_s(\mathbf{\Pi}_u^f)\mathrm{diag}_s(\mathbf{\Omega}_u^f)}\right). \quad (37)$$

and the Lagrange multiplier β_u^f is selected to meet the power budget of the transmitter on the forward direction.

Following the routine in [17], we can prove that the game (10) converges to its NE under sequential update by constructing a non-decreasing and upper-bounded Lyapunov function of precoding matrices (we omit the proof due to space limitation).

Theorem 3: Under the sequential (Gauss-Seidel) iterations, the game (10) converges to its NE.

V. Simulation Results

In this section, using Matlab, we numerically evaluate the performance of the above centralized and distributed algorithms. The simulation results are averaged over 20 runs. The number of antennas per node is 4. Transmit power $P_{\max} = 200$ mW for all nodes. Channel bandwidth is 4 MHz. Noise floor over the whole bandwidth is set as -94dBm. The channel fading is flat with a free-space attenuation factor of 2. The spreading angles of the signal at the receive antennas are from $-\pi/5$ to $\pi/5$. The close-in distance is 1 m.

A. Two Interfering FD-MIMO Links

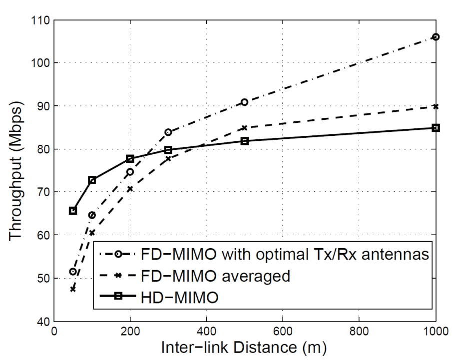

Fig. 3. Throughput of FD-MIMO (with and without Tx/Rx antenna selection) vs. HD-MIMO in exhaustive search case.

We first simulate a small-size network of 2 links while performing exhaustive search for the optimal FD-MIMO operational mode. To change the level of interference between the transmitter and receivers between two links, we vary the distance between two links. Using the centralized algorithm, Figure 3 depicts the network-throughput of the distributed algorithm using hierarchical game (namely FD-MIMO with optimal Tx/Rx antennas); network-throughput averaged over all possible FD-MIMO operational modes of the two links (namely FD-MIMO without Tx/Rx antennas); and network-throughput when two links operate in HD-MIMO mode (namely HD-MIMO). When the distances between two links are small, HD-MIMO mode surprisingly outperforms all FD-MIMO modes. This is because when the interference between nodes is severe (closer distance between the two links), it is more helpful to use all of available antennas to tune radiation patterns to avoid interfering unintended receivers. When the distance between two links increases, i.e, less interference, the FD-MIMO mode yields the higher throughput than HD-MIMO. For all considered distances between the two links, FD-MIMO with optimized Tx/Rx antenna has higher throughput than other FD-MIMO configurations.

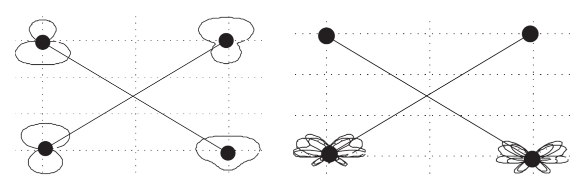

(a) FD-MIMO radiation patterns (b) HD-MIMO radiation patterns

Fig. 4. Antenna radiation patterns of FD-and HD-MIMO transmitters.

A snapshot of the radiation patterns of FD-MIMO and HD-MIMO using the above distributed algorithm is shown in Figure 4. As can be seen, by splitting the available antennas, links can afford to operate in FD-MIMO mode (with less number of antennas per transmitter) at the expense of incurring higher network interference (more interference beams visually pointing to unintended receivers). However, in HD-MIMO with a higher number of Tx antennas, HD-MIMO transmitter can configure its radiation patterns so as to cause less network interference.

Table I records the transmit power of FD-MIMO (with optimal Tx/Rx antenna selection), HD-MIMO with and without the developed pricing policy. Without the pricing policy, each FD-MIMO node uses all of its power budget $P_{\max}$ to transmit. The pricing policy discourages both FD- and HD-MIMO transmitters from injecting interference into the network. This makes them not willing to use all of their power budget. When pricing is used, we can see that HD-MIMO mode uses higher transmit power than FD-MIMO. This is because HD-MIMO node with higher number of antennas is more capable in controlling its beams to reduce the price (i.e., interference), allowing them to transmit with higher power than FD-MIMO transmitters.

TABLE I
Transmit power per node of HD-MIMO and FD-MIMO (in mW).

Node	FD-MIMO with pricing	FD-MIMO without pricing	HD-MIMO with pricing
1	122.48	200	152.89
2	93	200	0
3	2.2	200	0
4	108.2	200	196.33
Total (mW)	325.88	800	349.232

B. Network of Interfering FD-MIMO Links

We now simulate a FD-MIMO network of 6 links in a square field of 1000 m $\times$ 1000 m. Snapshots of the network with its radiation patterns under distributed and centralized FD-/HD-MIMO with and without the pricing policy are shown in Figure 5. We can observe that HD-MIMO transmitters are doing a better job than FD-MIMO nodes in steering their beams from neighboring unintended receivers.

The network-throughput vs. iterations is plotted in Figure 6. As can be seen, the network throughput under the distributed

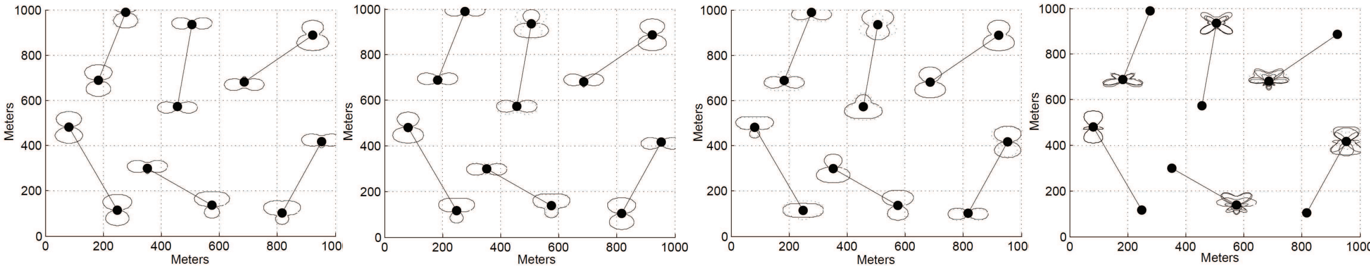

(a) FD-MIMO without pricing (b) FD-MIMO with pricing (c) Centralized FD-MIMO (d) Centralized HD-MIMO

Fig. 5. Antenna radiation patterns of FD- and HD-MIMO.

algorithm with pricing converges to that obtained with the centralized algorithm for both FD- and HD-MIMO. Averaging over all obtained locally optimal points, HD-MIMO operational mode significantly outperforms FD-MIMO mode. Even without the pricing policy, (greedy cases) HD-MIMO is also to preferable to FD-MIMO. This is because in greedy cases, all 12 FD-MIMO transmitters inject $12 \times 200 = 2400$ mW into the network, compared with $6 \times 200 = 1200$ mW of 6 HD-MIMO transmitters. In other words, receivers under FD-MIMO are likely to be more interfered than those in HD-MIMO networks.

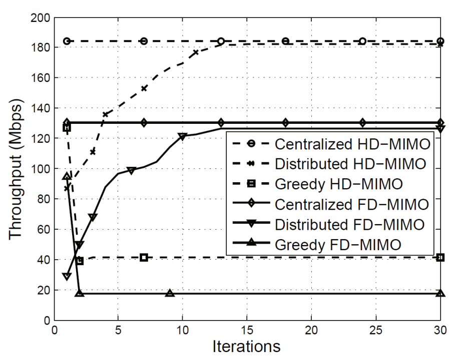

Fig. 6. Throughput of FD-MIMO and HD-MIMO vs. iterations.

To improve network throughput, antennas which induce too much interference should be switched off (i.e., allocated zero or very small power). To investigate how efficient antennas are used under FD- and HD-MIMO modes, Table II records the average number of unused antennas (those are allocated less than 10^{-7} mW). Without pricing, i.e., acting in a greedy manner, no antenna is turned off. When pricing is used to penalize transmitters with high interference, more antennas are switched off for FD-MIMO, compared with HD-MIMO. This is because HD-MIMO with higher number of antennas are better in managing network interference. For the smaller field 100×100 with severer network interference, more antennas are switched off, compared with the case of larger field 1000×1000.

TABLE II
NUMBER OF UNUSED ANTENNAS OF FD-MIMO AND HD-MIMO.

Network Scenario	Centralized FD	Greedy FD	Distributed FD	Centralized HD
100×100	18.6	0	17.3	7.9
1000×1000	16.2	0	15.7	4.1

VI. CONCLUSIONS

We have shown that Tx/Rx antenna selection has great potential in improving throughput of a single FD-MIMO link. Using game theory, pricing, and optimization theory, we designed both centralized and distributed algorithms that maximize throughput of a FD-MIMO network. Interestingly, under interfering scenarios, FD-MIMO does not always result in higher spectral efficiency than HD-MIMO. Instead, when links are strongly interfering, for the same number of RF-chains/antennas, HD-MIMO is preferable thanks to its better capability in controlling radiation beams. We believe this work is just the very first step in understanding how to properly exploit the latest advances of FD-MIMO in a network context. An interesting future work is to study whether the above observations hold if a device can transmit and receive simultaneously on the same MIMO antenna array.

REFERENCES

[1] J. I. Choi, M. Jain, K. Srinivasan, P. Levis, and S. Katti, "Achieving single channel, full duplex wireless communication," in *Proceedings of MobiCom Conference*, 2010, pp. 1–12.
[2] M. Jain, J. I. Choi, T. Kim, D. Bharadia, S. Seth, K. Srinivasan, P. Levis, S. Katti, and P. Sinha, "Practical, real-time, full duplex wireless," in *Proceedings of MobiCom Conference*, 2011, pp. 301–312.
[3] D. Bharadia, E. McMilin, and S. Katti, "Full duplex radios," in *Proceedings of SIGCOMM Conference*, 2013.
[4] V. Aggarwal, M. Duarte, A. Sabharwal, and N. Shankaranarayanan, "Full- or half-duplex? a capacity analysis with bounded radio resources," in *IEEE Information Theory Workshop (ITW)*, 2012, pp. 207–211.
[5] E. Aryafar, M. A. Khojastepour, K. Sundaresan, S. Rangarajan, and M. Chiang, "MIDU: enabling MIMO full duplex," in *Proceedings of MobiCom Conference*, 2012, pp. 257–268.
[6] B. Chen, V. Yenamandra, and K. Srinivasan, "Flexradio: Fully flexible radios," The Ohio State University, Tech. Rep., 2013. [Online]. Available: http://www.cse.ohio-state.edu/~kannan/cosyne/nsdi14-anyduplex.pdf
[7] B. Day, A. Margetts, D. Bliss, and P. Schniter, "Full-duplex MIMO relaying: Achievable rates under limited dynamic range," *IEEE Journal on Selected Areas in Communications*, vol. 30, no. 8, pp. 1541–1553, 2012.
[8] T. M. Kim, H. J. Yang, and A. Paulraj, "Distributed sum-rate optimization for full-duplex MIMO system under limited dynamic range," *IEEE Signal Processing Letters*, vol. 20, no. 6, pp. 555–558, 2013.
[9] Q. Li, K. Li, and K. Teh, "Achieving optimal diversity-multiplexing trade-off for full-duplex MIMO multihop relay networks," *IEEE Transactions on Information Theory*, vol. 57, no. 1, pp. 303–316, 2011.
[10] D. P. Bertsekas, *Nonlinear Programming*. Athena Scientific, 1995.
[11] S. Boyd and L. Vandenberghe, *Convex Optimization*. Cambridge University Press, 2004.
[12] M. J. Osborne, *An Introduction to Game Theory*. Oxford University Press, 2004.
[13] D. Nguyen and M. Krunz, "Spectrum management and power allocation in MIMO cognitive networks," in *Proc. of the INFOCOM Conf.*, 2012, pp. 412–420.
[14] A. W. Marshall and I. Olkin, *Inequalities: Theory of Majorization and Its Applications*. Academic Press, 1979.
[15] D. Hoang and R. Iltis, "Noncooperative eigencoding for MIMO ad hoc networks," *IEEE Trans. on Signal Processing*, vol. 56, no. 2, pp. 865–869, 2008.
[16] R. A. Horn and C. R. Johnson, *Matrix Analysis*. Cambridge University Press, 1990.
[17] D. Nguyen and M. Krunz, "Spectrum management and power allocation in MIMO cognitive networks," University of Arizona, Tech. Rep. TR-UA-ECE-2011-2, August 2011. [Online]. Available: http://www.ece.arizona.edu/~krunz